To appear in *The Astrophysical Journal Letters*

Evidence for a Black Hole and Accretion Disk in the LINER NGC 4203[1]

Joseph C. Shields[2], Hans-Walter Rix[3], Daniel H. McIntosh[4], Luis C. Ho[5], Greg Rudnick[4], Alexei V. Filippenko[6], Wallace L. W. Sargent[7], and Marc Sarzi[3,8]

ABSTRACT

We present spectroscopic observations from the *Hubble Space Telescope* that reveal for the first time the presence of a broad pedestal of Balmer-line emission in the LINER galaxy NGC 4203. The emission-line profile is suggestive of a relativistic accretion disk, and is reminiscent of double-peaked transient Balmer emission observed in a handful of other LINERs. The very broad line emission thus constitutes clear qualitative evidence for a black hole, and spatially resolved narrow-line emission in NGC 4203 can be used to constrain its mass, $M_{BH} \leq 6 \times 10^6$ $M_\odot$ at 99.7% confidence. This value implies a ratio of black-hole mass to bulge mass $\lesssim 7 \times 10^{-4}$ in NGC 4203, which is less by a factor of $\sim 3 - 9$ than the mean ratio obtained for other galaxies.

The availability of an independent constraint on central black-hole mass makes NGC 4203 an important testbed for probing the physics of weak active galactic nuclei (AGNs). Assuming M_{BH} near the detection limit, the ratio of observed luminosity to the Eddington luminosity is $\sim 10^{-4}$. This value is consistent with advection-dominated accretion, and hence with scenarios in which an ion torus irradiates an outer accretion disk that produces the observed double-peaked line emission. Follow-up observations will make it possible to improve the black-hole mass estimate and study variability in the nuclear emission.

Subject headings: galaxies: active — galaxies: individual (NGC 4203) — galaxies: nuclei — galaxies: Seyfert

---

[1]Based on observations with the *Hubble Space Telescope* obtained at STScI, which is operated by AURA, Inc., under NASA contract NAS5-26555.

[2]Physics & Astronomy Department, Ohio University, Athens, OH 45701; shields@phy.ohiou.edu

[3]Max-Planck-Institut für Astronomie, Königstuhl 17, Heidelberg, D-69117, Germany; rix@mpia-hd.mpg.de

[4]Steward Observatory, University of Arizona, Tucson, AZ 85721; dmac, grudnick@as.arizona.edu

[5]The Observatories of the Carnegie Institution of Washington, 813 Santa Barbara St., Pasadena, CA 91101-1292; lho@ociw.edu

[6]Astronomy Department, University of California, Berkeley, CA 94720-3411; alex@astro.berkeley.edu

[7]Palomar Observatory, Caltech 105-24, Pasadena, CA 91125; wws@astro.caltech.edu

[8]Dipartimento di Astronomina, Università di Padova, vicolo dell'Osservatorio 5 I-35122, Italy; sarzi@pd.astro.it

1. Introduction

Spectroscopic surveys have revealed that a large fraction of nearby early-type galaxies harbor low-ionization nuclear emission-line regions, or LINERs (Heckman 1980; Ho et al. 1997a and references therein). The physical understanding of these sources remains rudimentary, but there are strong indications that at least some LINERs are weak versions of the Seyfert or QSO phenomenon, and hence powered by accretion onto a massive black hole. LINERs are nonetheless distinct from classical AGNs in terms of their characteristic (low) luminosity, emission-line properties, and broad-band spectral energy distribution (Ho 1999). These differences may follow from fundamental disparities in the accretion process operative in luminous and weak AGNs.

The study of emission-line behavior on small spatial scales within galaxy nuclei provides one strategy for probing the energetics, dynamics, and structure of LINERs and related objects. Here we report on observations acquired with the *Hubble Space Telescope* (*HST*) for the LINER NGC 4203. The data provide dynamical constraints on a black hole, and reveal line emission that may directly trace an accretion flow in this source. These observations and future follow-up studies will provide an important framework for testing physical models for the structure of LINERs, and the nature of black holes in galaxy nuclei.

2. Observations

NGC 4203 was observed with the Space Telescope Imaging Spectrograph (STIS) as part of a spectroscopic survey of nearby weakly active galaxy nuclei. The full details of this program will be reported elsewhere (Rix et al., in preparation). NGC 4203 is of S0 morphological type, seen nearly face-on, and its nucleus was classified spectroscopically by Ho et al. (1997b) as a LINER 1.9 source. NGC 4203 exhibits a recession velocity of 1088 km s^{-1}, and we assume a distance for this source of 9.7 Mpc (Tully 1988).

HST observations were acquired on 1999 April 18 UT, with the $0\farcs2 \times 52''$ slit placed across the nucleus at position angle (PA) = 105.6°. Two exposures totaling 1630 s and three exposures totaling 2779 s were obtained with the G430L and G750M gratings, resulting in spectra spanning 3300 – 5700 Å and 6300 – 6850 Å with full width at half maximum (FWHM) spectral resolution for extended sources of 10.9 and 2.2 Å, respectively. The telescope was offset by $0\farcs05$ ($\approx$ 1 pixel) along the slit direction between repeated exposures. The two-dimensional (2-D) spectra were bias- and dark-subtracted, flat-fielded, shifted to a common alignment, combined with repeated exposures to obtain single blue and red spectra, cleaned of residual cosmic rays and hot pixels, and corrected for geometrical distortion. The data were wavelength- and flux-calibrated via standard STSDAS procedures.

3. Results

3.1. The Unresolved Nucleus

Spectra of the nucleus of NGC 4203, obtained by coadding the 2-D spectra over the central 0.″25 along the slit, are shown in Figure 1. This extraction width represents approximately twice the FWHM for the STIS point-spread function (PSF; i.e., FWHM = 0.″12). The data show strong, low-ionization forbidden line emission, consistent with the classification of this source as a LINER. The red spectrum displays an additional striking feature in the form of a distinct broad component of Hα, which contributes prominent high-velocity shoulders to the line profile. Ground-based observations of this source obtained with the Palomar 5-m telescope in 1985 and reported by Ho et al. (1997c) also show evidence of broad Hα emission, but in the earlier spectrum the broad component is well represented by a Gaussian profile with a FWHM of 1500 km s^{-1}, far less than the velocity difference of $\sim$ 7200 km s^{-1} between the profile shoulders evident in Figure 1*a*.

We examined the properties of the broad Hα emission in more detail by removing the narrow contributions to the blended line. A synthetic profile for the narrow emission was constructed from the [S II] $\lambda\lambda$6716, 6731 lines, and used to model the lines of [N II] $\lambda\lambda$6548, 6583, and narrow Hα. The overall emission feature has a central core that strongly resembles the broad Hα line seen previously in the Palomar spectrum, and we consequently included such a component of "normal" broad-line emission, matched to the profile parameters and redshift of the ground-based observation, while fitting the overall blend. The [N II] doublet was constrained to the flux ratio of 1:3.0 predicted by atomic parameters, and the line strengths were otherwise adjusted in order to produce the smoothest residual profile.

Removal of the narrow lines and central peak of broad Hα emission results in the Hα line profile shown at the bottom of Figure 1*a*. The profile of the remaining broad pedestal in the 6540 – 6590 Å region is sensitive to the details of the decomposition; however, the profile remains distinctly double-peaked, independent of the scaling for the subtracted components. The broad feature has a full-width near zero intensity of at least 12,500 km s^{-1}, and a total flux of $\sim 1.2 \times 10^{-13}$ erg s^{-1} cm^{-2}. The line appears centered near the narrow-line redshift, although the profile of the broad feature is highly asymmetric, with stronger emission in the blue peak and a more extended wing on the red side. Similar emission is clearly visible in the profile of the Hβ feature (Fig. 1*b*).

The scaling of the "normal" broad Hα component employed in the profile decomposition is 84% that seen in the earlier Palomar observation, which represents reasonable agreement when allowance is made for photometric uncertainties in the ground-based data and ambiguities in the fitting procedure. The degree to which the broad wings have varied is of considerable interest, given the variability of double-peaked emission reported in some other LINERs (e.g., Storchi-Bergmann, Baldwin, & Wilson 1993; Halpern & Eracleous 1994; Bower et al. 1996). To address this question, we conducted tests of the observability of extended Hα wings in the Palomar spectrum. Shoulders on the Hα profile resembling those in the *HST* data might have eluded detection in the Palomar

spectrum if this component was present in 1985, due to wavelength-dependent focus variations and the strong stellar continuum measured through the relatively large ($2''\times 4''$) ground-based effective aperture.

Since we cannot say for sure whether the broad shoulders on the Balmer lines were present in 1985, it is unclear whether the appearance of this emission in 1999 represents a transient event or a more stable attribute of NGC 4203. The fact that the central core of emission has remained roughly constant suggests that the central source has not changed appreciably, in which case the detection of the broad pedestal of emission probably results primarily from the diminished contamination by starlight in the *HST* aperture, rather than intrinsic variability. *HST* has revealed similar behavior in NGC 4450, observed as part of our survey (Ho et al. 2000a). The fact that *two* sources out of a relatively small sample of objects surveyed (24 galaxies total, of which 8 are LINERs) were discovered to have double-peaked emission lines suggests that small-aperture spectroscopy is an important complement to variability studies for uncovering this phenomenon in LINERs.

3.2. Gas Kinematics and Mass Modeling

The 2-D spectra of NGC 4203 exhibit spatially resolved narrow emission, which is most readily apparent in Hα and the [N II] lines. These features are detected out to a distance of $\sim 1''$ (47 pc) in both directions from the nucleus. Line fluxes and radial velocities were measured as a function of position along the slit, by performing a simultaneous fit with χ^2 minimization, assuming Gaussian line profiles. The [S II] lines are visible interior to $\pm 0\farcs5$ from the nucleus, and are included in the fits for that region. The [O I] $\lambda\lambda$6300, 6364 lines are prominent in the nucleus but were not included in the fits; emission in these lines is highly concentrated spatially, and the [O I] profiles are also distinctly broader than those of the other forbidden lines in the red spectrum (consistent with linewidth vs. critical density correlations reported for other LINERs; e.g., Filippenko & Halpern 1984). The continuum underlying the emission features was represented by a straight line, and for columns near the nucleus the broad Hα emission feature was represented by the combination of three Gaussian profiles, which was successful in isolating the narrow-line emission.

The radial velocity of the narrow-line gas is plotted as a function of position in the top panel of Figure 2. A distinct gradient is seen through the central $\pm 0\farcs5$, which is steepest in the innermost $\pm$ $0\farcs1$. Velocities level off and show evidence of a significant decline in amplitude at larger distances, possibly due to a warp in the gas disk.

The measurements illustrated in Figure 2 make it possible to probe the central mass distribution in this galaxy, which is of particular interest given the activity seen in the nucleus. With only one slit position, a number of assumptions are necessary to obtain a well-constrained kinematic model. Here, we assumed (1) that the gas is orbiting the nucleus in a coplanar disk at the local circular velocity, (2) the *stellar* mass-to-light ratio Υ is spatially constant and the stellar orbit distribution is approximately isotropic, and (3) the stars dominate the total mass inside a $1\farcs5 \times 4''$

aperture (see Sarzi et al. 2000 for a thorough description of the modeling). We then used the acquisition image taken with STIS to derive the deprojected, PSF-corrected light distribution: it is well described by a cusp with $\rho_*(r) \propto r^{-1.55}$ and a central, presumably nonstellar point source. Using the isotropic, spherical Jeans equation, we can predict from $\rho_*(r)$ the stellar velocity dispersion σ_* over a $1\farcs5 \times 4''$ aperture as a function of Υ; matching the observed $\sigma_* = 124$ km s^{-1} within this aperture (Dalle Ore et al. 1991) then dictates the value of Υ, to which we assign a 30% error bar reflecting the geometrical uncertainties in this derivation. For any assumed M_{BH} one can then solve for the combination of disk inclination and disk major axis that best matches the data. The lines in the bottom panel of Figure 2 represent such a model sequence in M_{BH} where the disk orientation was chosen to optimize the match to the data. While the ultra-broad Hα emission implies the presence of a black hole, the formal best fit to the extended rotation curve is for a small black-hole mass (i.e., χ^2 is minimized at $M_{BH} = 0$ M$_\odot$). We thus obtain a formal upper limit of $M_{BH} \leq 6 \times 10^6$ M$_\odot$ at 99.7% confidence.

Examination of an archival WFPC2 V-band image reveals asymmetric patchy absorption suggestive of an inclined ($\sim 50°$) dusty disk with a major-axis PA of $\sim 0°$. If this orientation applies to the nebular gas (as suggested by *HST* imaging studies of other LINERs; Pogge et al. 2000), our slit PA is $\sim 15 \pm 20°$ from the disk minor axis. Over this PA range the projection factors change dramatically, and we cannot use the dust lane information directly to constrain M_{BH}. Formally, the χ^2 obtained with minor axis PA = 15° is much worse than for the best fit above. We thus must await spectra at additional PAs or offsets from the nucleus in order to obtain more direct constraints on the disk orientation and black-hole mass (e.g., Bower et al. 1998).

4. Discussion

4.1. The Black Hole and its Galactic Host

Studies of the velocity field for stars and occasionally gas in the centers of nearby bulge-dominated galaxies have generated a list of strong candidates for supermassive black holes (e.g., Kormendy & Richstone 1995; Ho 1998). These studies increasingly suggest that the black-hole mass is correlated with the mass of the stellar bulge in the host galaxy. We consequently examined the black-hole mass in relation to the bulge mass in the case of NGC 4203. This galaxy has a total apparent magnitude of $B_T = 11.61$, with $B - V = 0.97$ (de Vaucouleurs et al. 1991). Burstein (1979) decomposed the B-band photometric profile of NGC 4203 into an exponential disk and $r^{1/4}$-law bulge, and obtained a disk/bulge luminosity ratio of 2.0. For a representative mass-to-light ratio of $\Upsilon_V \approx 6$, the corresponding bulge mass is $\sim 9 \times 10^9$ M$_\odot$; our upper limit of $M_{BH} \leq 6 \times 10^6$ M$_\odot$ thus implies a black-hole/bulge mass ratio of $\lesssim 7 \times 10^{-4}$. Although this number is rather uncertain, it falls near the low end of previous estimates for normal galaxies ($\sim$0.002 – 0.006; Magorrian et al. 1998; van der Marel 1998) and overlaps with estimates derived from reverberation measurements of Seyfert nuclei (Wandel 1999). A measurement or more stringent limit on M_{BH} in NGC 4203

would be of interest for gauging whether the black-hole/bulge correlation applies in this source.

4.2. The Black Hole and its AGN

The luminous output of the LINER in NGC 4203 can be used as a diagnostic of accretion onto the central black hole. Ho et al. (2000b) have quantified the broad-band spectral energy distribution for this source, and estimate a total bolometric luminosity for the nucleus of 9.5×10^{40} erg s^{-1}. For the limit on M_{BH} obtained from the nebular rotation curve, this result implies a ratio to the Eddington luminosity of $L/L_{Edd} \gtrsim 1 \times 10^{-4}$.

This result and the broad Balmer profiles in the NGC 4203 nucleus have an appealing consistency in the framework of advection-dominated accretion flow (ADAF) models for accretion onto the central black hole. ADAFs are expected to occur naturally in systems with relatively low accretion rates (e.g., see Narayan, Mahadevan, & Quataert 1998 for a review). For an α-disk prescription for the accretion flow, an ion torus will form in the inner disk, and advect a significant fraction of the accretion energy into the black hole, when the accretion rate falls below a critical value, $\dot{M}_{crit} \approx \alpha^2 \dot{M}_{Edd}$. Here the Eddington accretion rate is defined so that $L_{Edd} = 0.1\,\dot{M}_{Edd}\,c^2$. Adopting a plausible value of $\alpha \approx 0.3$ implies that $\dot{M}_{crit} \approx 0.1\dot{M}_{Edd}$, corresponding to $L \approx 0.1 L_{Edd}$, below which the luminosity is expected to scale as $\dot{M}^2$. The limiting value of L/L_{Edd} in NGC 4203 is in the advection-dominated regime, and corresponds to an accretion rate $\dot{M} \approx 5 \times 10^{-4} M_\odot$ yr^{-1}; an improved constraint on M_{BH} is of obvious interest for testing this physical picture.

ADAFs can account for many properties of luminous radio galaxies, which often resemble NGC 4203 in displaying broad, double-peaked Balmer emission lines (Eracleous & Halpern 1994). These profiles have been modeled in terms of a relativistic disk (Chen & Halpern 1989), with predicted properties notably similar to those seen in NGC 4203 – specifically, stronger emission in the blue peak than in the red, and a sharper cutoff to the blue shoulder than in the red. The line emission presumably arises from an outer part of the accretion flow that remains geometrically thin and may be irradiated by the inner ion torus that is characteristic of ADAFs. Modeling of the emission profile can potentially yield an estimate of the radius at which the transition from thin disk to ion torus occurs, and we defer more detailed exploration of this possibility to a later paper.

Alternative explanations exist for the double-peaked Balmer lines. Possibilities include emission from bipolar outflows or anisotropically illuminated clouds, from gas surrounding binary black holes, or from a tidally disrupted star or other asymmetric circumnuclear structure (Eracleous et al. 1999 and references therein). Studies of double-peaked emission profiles in other LINERs have revealed evolution in the profiles over time, and such observations can potentially be used to distinguish between these possibilities, and to probe the structure of the accretion flow if a disk is in fact responsible. In the case of NGC 1097, variations in the relative heights of the red and blue line peaks are suggestive of emission from an orbiting ring that is azimuthally asymmetric in its emissivity (Storchi-Bergmann et al. 1997). If the elevated blue wing in NGC 4203 arises from an

asymmetry of this type, we might expect the peak in emission to eventually oscillate to the red wing. If the timescale for the asymmetry to propagate matches the orbital timescale, then we can predict a rise in the red wing in $\lesssim 4$ years, based on the velocity width of the emission-line shoulders and our bound on the black-hole mass. Periodic variability on other (probably longer) timescales may be relevant if the asymmetry propagates as a wave or via precession. Follow-up observations thus may yield further important constraints on the structure and evolution of the accretion disk.

5. Conclusions

NGC 4203 is the latest addition to a small set of LINERs that exhibit broad, double-shouldered Balmer lines. The discovery of two such objects in our *HST* survey (NGC 4450 being the other; Ho et al. 2000a) suggests that such emission may be common in LINERs, but often eludes detection in ground-based apertures for which the contrast with the stellar continuum is weak. The line profile in NGC 4203 is noteworthy for its resemblance to emission profiles seen in broad-line radio galaxies, which have been interpreted as the signature of a thin outer accretion disk irradiated by an inner ion torus, representing an advection-dominated flow onto a black hole.

The nucleus of NGC 4203 also exhibits spatially resolved emission that can be used to provide kinematic information on the underlying mass distribution. The existing observations at a single PA can be used to restrict the underlying black-hole mass to $M_{BH} \leq 6 \times 10^6$ $M_\odot$. The availability of a mass estimate for the black hole is of fundamental importance for studying the physics of the accretion process. Our limiting value for M_{BH} is consistent with a sub-Eddington accretion rate and formation of an ADAF, although a more stringent limit could challenge this picture. Follow-up observations from space, or with small apertures under good seeing conditions on the ground, will make it possible to improve the estimate of the black-hole mass and study time evolution of the broad Hα emission.

This research was supported financially through NASA grant NAG 5-3556, and by GO-07361-96A, awarded by STScI, which is operated by AURA, Inc., for NASA under contract NAS5-26555. We thank T. Statler for helpful discussions, and the referee, M. Eracleous, for valuable comments.

REFERENCES

Bower, G. A., et al. 1998, ApJ, 492, L111

Bower, G. A., Wilson, A. S., Heckman, T. M., & Richstone, D. O. 1996, AJ, 111, 1901

Burstein, D. 1979, ApJ, 234, 435

Chen, K., & Halpern, J. P. 1989, ApJ, 344, 115

Dalle Ore, C., Faber, S. M., Jesús, J., Stoughton, R., & Burstein, D. 1991, ApJ, 366, 38

de Vaucouleuers, G., de Vaucouleuers, A., Corwin, H. G., Buta, R. J., Paturel, G., & Fouqué, P. 1991, Third Reference Catalogue of Bright Galaxies (New York: Springer)

Eracleous, M. 1999, in ASP Conf. Ser. 175, Structure and Kinematics of Quasar Broad Line Regions, eds. C. M. Gaskell et al. (San Francisco: ASP), 163

Eracleous, M., & Halpern, J. P. 1994, ApJS, 90, 1

Filippenko, A. V., & Halpern, J. P. 1984, ApJ, 285, 458

Halpern, J. P., & Eracleous, M. 1994, ApJ, 433, L17

Heckman, T. M, 1980, A&A, 87, 152

Ho, L. C. 1998, in Observational Evidence for Black Holes in the Universe, ed. S. K. Chakrabarti (Dordrecht: Kluwer), 157

Ho, L. C. 1999, ApJ, 516, 672

Ho, L. C., Filippenko, A. V., & Sargent, W. L. W. 1997a, ApJ, 487, 568

Ho, L. C., Filippenko, A. V., & Sargent, W. L. W. 1997b, ApJS, 112, 315

Ho, L. C., Filippenko, A. V., & Sargent, W. L. W. 1997c, ApJS, 112, 391

Ho, L. C., Rudnick, G., Rix, H.-W., Shields, J. C., McIntosh, D. H., Filippenko, A. V., Sargent, W. L. W., & Eracleous, M. 2000a, ApJ, submitted

Ho, L. C., et al. 2000b, in preparation

Kormendy, J., & Richstone, D. 1995, ARA&A, 33, 581

Magorrian, J., et al. 1998, AJ, 115, 2285

Narayan, R., Mahadevan, R., & Quataert, E. 1998, in The Theory of Black Hole Accretion Discs, eds. M. A. Abramowicz et al. (Cambridge: Cambridge Univ. Press), 148

Pogge, R. W., Maoz, D., Ho, L. C., & Eracleous, M. 2000, ApJ, in press (astro-ph/9910375)

Sarzi, M., Rix, H.-W., Shields, J. C., Ho, L. C., Rudnick, G., McIntosh, D. H., Filippenko, A. V., & Sargent, W. L. W. 2000, in preparation

Storchi-Bergmann, T., Baldwin, J. A., & Wilson, A. S. 1993, ApJ, 410, L11

Storchi-Bergmann, T., Eracleous, M., Ruiz, M. T., Livio, M., Wilson, A. S., & Filippenko, A. V. 1997, ApJ, 489, 87

Tully, R. B. 1988, Nearby Galaxies Catalog (Cambridge: Cambridge Univ. Press)

van der Marel, R. P. 1998, in IAU Symposium 186, Galaxy Interactions at Low and High Redshift, ed. D. B. Sanders & J. Barnes (Dordrecht: Kluwer), 333

Wandel, A. 1999, ApJ, 519, L39

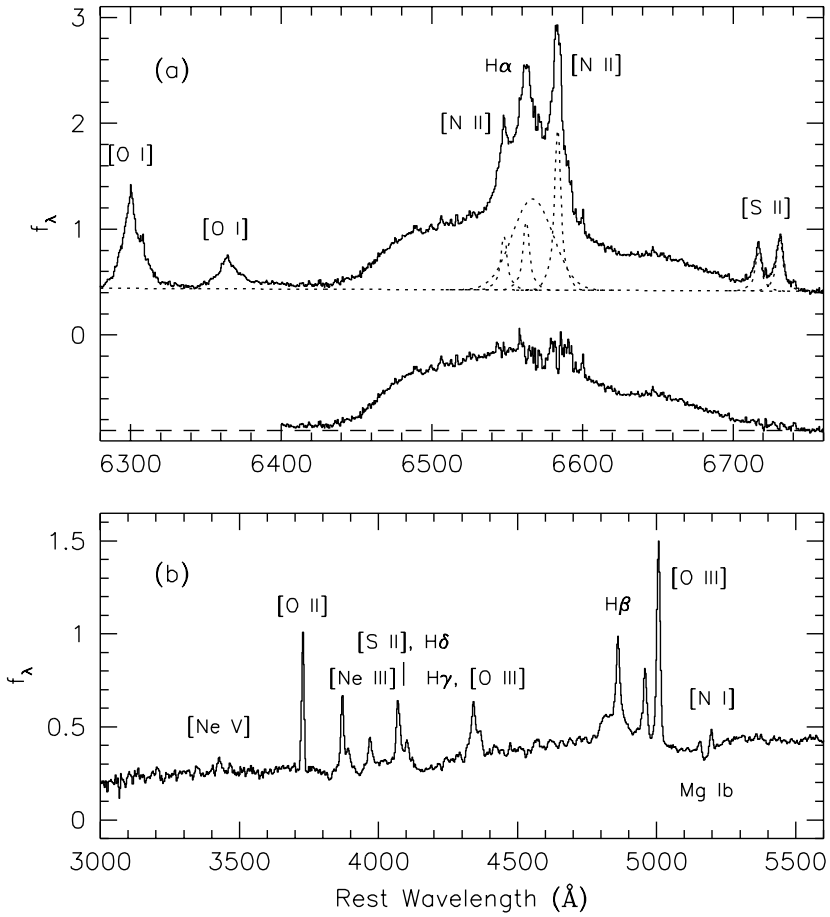

Fig. 1.— STIS spectra of the nucleus of NGC 4203, acquired with the (*a*) G750M and (*b*) G430L gratings. Flux densities are in units of 10^{-15} erg s^{-1} cm^{-2} Å^{-1}. The dotted curves in (*a*) show model components adopted for the continuum, narrow lines, and "normal" broad Hα emission. Subtraction of these components yields the residual broad feature shown at the bottom of the panel.

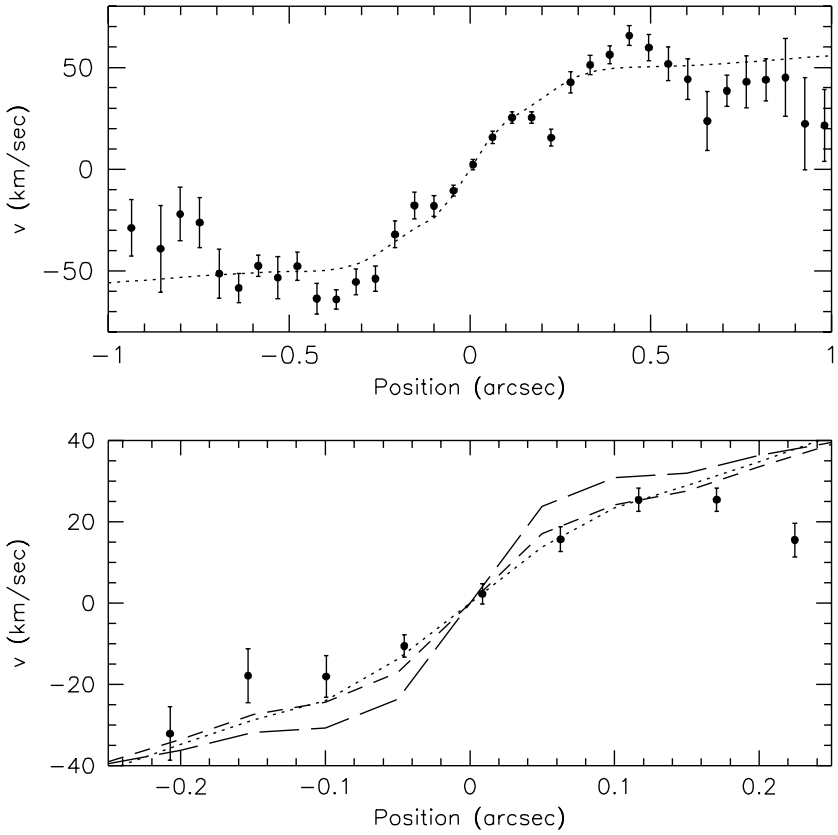

Fig. 2.— *Top panel:* Emission-line gas velocity as a function of position along the slit, measured relative to the nucleus. Points represent the measured values, and the dotted line shows the best-fitting model rotation curve with no black hole. *Bottom panel:* Expanded view of the central rotation curve. The lines represent predictions for the best-fitting model rotation curve with $M_{BH} =$ 0 $M_\odot$ (dotted line), 4.0×10^6 $M_\odot$ (short-dashed line), and 4.9×10^7 $M_\odot$ (long-dashed line). In each case, the model is constrained to reproduce the large-aperture stellar velocity dispersion (see text for further details). A χ^2 analysis for a family of such fits implies that $M_{BH} \leq 6 \times 10^6$ $M_\odot$ at 99.7% confidence.